Irreversibility, Loschmidt Echo, and Thermodynamic Uncertainty Relation

Yoshihiko Hasegawa*
Department of Information and Communication Engineering, Graduate School of Information Science and Technology, The University of Tokyo, Tokyo 113-8656, Japan

(Received 23 March 2021; accepted 28 October 2021; published 7 December 2021)

Entropy production characterizes irreversibility. This viewpoint allows us to consider the thermodynamic uncertainty relation, which states that a higher precision can be achieved at the cost of higher entropy production, as a relation between precision and irreversibility. Considering the original and perturbed dynamics, we show that the precision of an arbitrary counting observable in continuous measurement of quantum Markov processes is bounded from below by the Loschmidt echo between the two dynamics, representing the irreversibility of quantum dynamics. When considering particular perturbed dynamics, our relation leads to several thermodynamic uncertainty relations, indicating that our relation provides a unified perspective on classical and quantum thermodynamic uncertainty relations.

DOI: 10.1103/PhysRevLett.127.240602

Introduction.—A thermodynamic uncertainty relation (TUR) [1–17] (see [18] for a review) gives a universal relation between precision and thermodynamic cost. It states that $[\![J]\!]^2/\langle J\rangle^2 \geq 2/\langle\sigma\rangle$, where $\langle J\rangle$ and $[\![J]\!]$ are the mean and standard deviation, respectively, of a current observable J, and $\langle\sigma\rangle$ is the mean of the entropy production. The TUR indicates that a higher precision can be achieved at the cost of higher entropy production. The entropy production quantifies the irreversibility of a system. Let $\mathcal{P}_F(\Gamma)$ be the probability for observing a trajectory Γ in the forward process and $\mathcal{P}_R(\bar{\Gamma})$ be the probability for observing a time-reversed trajectory $\bar{\Gamma}$ in the reversed process. Then, the entropy production is defined by a log ratio between $\mathcal{P}_F(\Gamma)$ and $\mathcal{P}_R(\bar{\Gamma})$ [Fig. 1(a)]: $\langle\sigma\rangle = D[\mathcal{P}_F(\Gamma)||\mathcal{P}_R(\bar{\Gamma})] \equiv \langle \ln[\mathcal{P}_F(\Gamma)/\mathcal{P}_R(\bar{\Gamma})]\rangle$, where $D[\bullet||\bullet]$ denotes the relative entropy. This relation suggests that the TUR is a consequence of irreversibility, i.e., the larger the extent of irreversibility, the higher the precision of a thermodynamic machine.

In Newtonian dynamics, despite microscopic reversibility, irreversibility emerges due to the chaotic nature of many-body systems. For chaotic systems, even considering reversed dynamics by reversing the sign of the momenta, an infinitely small perturbation applied to the state yields an exponential divergence from the original reversed dynamics, indicating the infeasibility of such reversed dynamics. Thus, the extent of irreversibility can be evaluated through the extent of chaos, which is often quantified by the Lyapunov exponent in classical dynamics. The Loschmidt echo [19–21] is an indicator for the effect of small perturbations applied to the Hamiltonian in quantum systems. It can be viewed as a quantum analog of the Lyapunov exponent. Consider an isolated quantum system. Given an initial pure state $|\Psi(0)\rangle$, with Hamiltonian H and perturbed Hamiltonian $H_\star$, the Loschmidt echo η is defined as follows:

$$\eta \equiv |\langle\Psi(0)|e^{iH_\star\tau}e^{-iH\tau}|\Psi(0)\rangle|^2. \tag{1}$$

Equation (1) evaluates the fidelity between two states, $e^{-iH\tau}|\Psi(0)\rangle$ and $e^{-iH_\star\tau}|\Psi(0)\rangle$, at time $t=\tau$, where $\tau>0$ [Fig. 1(b)]. These states are generated through the forward-time evolution induced by H and $H_\star$, respectively. Alternatively, Eq. (1) can be viewed as the fidelity between $|\Psi(0)\rangle$ and $e^{iH_\star\tau}e^{-iH\tau}|\Psi(0)\rangle$ at $t=0$, where the latter state is obtained by applying the forward-time evolution by H and the subsequent reversed-time evolution by $H_\star$ to $|\Psi(0)\rangle$ [Fig. 1(c)]. The second interpretation gives a natural extension to classical irreversibility. In this Letter, we show that the precision of any counting observable in the continuous measurement of quantum Markov processes is bounded from below by the Loschmidt echo. This relation can be viewed as a quantum extension of classical TURs. Notably, the obtained quantum TUR holds for any continuous measurement, which has not been achieved for previous quantum TURs [22–33]. When we consider empty dynamics for the perturbed dynamics, the main result appears to be reminiscent of a bound obtained in Ref. [30], whereas the bound in this Letter provides a tighter bound for a classical limit. Moreover, when we consider time-scaled perturbed dynamics, the main result reduces to the bound reported in Ref. [28], which covers a classical TUR comprising the dynamical activity [6]. Our result provides a unified perspective on classical and quantum TURs.

Results.—We consider a quantum Markov process described by a Lindblad equation [34,35]. Let $\rho_S(t)$ be a density operator at time t in the principal system S. The time evolution of $\rho_S(t)$ is governed by

 © 2021 American Physical Society

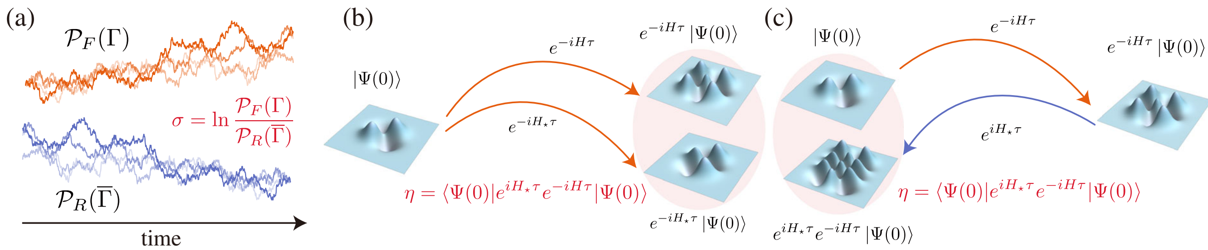

FIG. 1. Quantification of irreversibility. (a) Entropy production σ in classical Markov processes, defined by a log ratio between $\mathcal{P}_F(\Gamma)$, the probability for observing a trajectory Γ in the forward process, and $\mathcal{P}_R(\bar{\Gamma})$, the probability for observing a time-reversed trajectory $\bar{\Gamma}$ in the reversed process. (b) Loschmidt echo η in quantum dynamics, which is the fidelity between two states, $e^{-iH\tau}|\Psi(0)\rangle$ and $e^{-iH_\star\tau}|\Psi(0)\rangle$ at $t=\tau$. These states are obtained through forward-time evolution induced by H and $H_\star$, respectively. (c) An interpretation of the Loschmidt echo η as the fidelity between two states, $|\Psi(0)\rangle$ and $e^{iH_\star\tau}e^{-iH\tau}|\Psi(0)\rangle$, at $t=0$. The latter state is obtained through forward-time evolution by H and the subsequent reversed-time evolution by $H_\star$.

$$\dot{\rho}_S = \mathcal{L}\rho_S \equiv -i[H_S,\rho_S] + \sum_{m=1}^{M}\mathcal{D}(\rho_S, L_m), \tag{2}$$

where $\dot{\bullet}$ is the time derivative, $\mathcal{L}$ is a Lindblad superoperator, H_S is a Hamiltonian, $\mathcal{D}(\rho_S, L) \equiv L\rho_S L^\dagger - \{L^\dagger L, \rho_S\}/2$ is a dissipator, and L_m ($1 \le m \le M$ with M being the number of L_m) is the mth jump operator ($[\bullet,\bullet]$ and $\{\bullet,\bullet\}$ denote the commutator and anticommutator, respectively). Note that H_S is different from the total Hamiltonian H, which induces unitary time evolution in the total system. For a sufficiently small time interval Δt, Eq. (2) admits the Kraus representation $\rho_S(t+\Delta t) = \sum_{m=0}^{M} V_m \rho_S(t) V_m^\dagger$, where

$$V_0 \equiv \mathbb{I}_S - i\Delta t H_S - \frac{1}{2}\Delta t \sum_{m=1}^{M} L_m^\dagger L_m, \tag{3}$$

$$V_m \equiv \sqrt{\Delta t} L_m \qquad (1 \le m \le M). \tag{4}$$

Here, $\mathbb{I}_S$ denotes the identity operator in S (the other identity operators are defined similarly). V_0 corresponds to no jump and V_m ($1 \le m \le M$) to the mth jump within the interval $[t, t+\Delta t]$. V_m ($0 \le m \le M$) satisfies the completeness relation $\sum_{m=0}^{M} V_m^\dagger V_m = \mathbb{I}_S$. V_m defined in Eqs. (3) and (4) are not the only operators consistent with Eq. (2). There are infinitely many operators that can induce the same time evolution.

Using the input-output formalism [36–39], employed in studying TURs in a quantum domain [28,30], we describe the time evolution generated by the Kraus operators [Eqs. (3) and (4)] as interactions between the principal system S and environment E. Let $t=0$ and $t=\tau$ be the initial and final times of time evolution, respectively. We discretize the time interval $[0,\tau]$ by dividing it into N intervals, where N is a sufficiently large natural number; in addition, we define $\Delta t \equiv \tau/N$ and $t_k \equiv \Delta t k$ ($t_0 = 0$ and $t_N = \tau$). Here, the orthonormal basis of E is assumed to be $|m_{N-1},\ldots,m_1,m_0\rangle$ ($m_k \in \{0,1,\ldots,M-1,M\}$), where a subspace $|m_k\rangle$ interacts with S through a unitary operator U_{t_k} during an interval $[t_k, t_{k+1}]$ (Fig. 2). When the initial states of S and E are $|\psi_S\rangle$ and $|0_{N-1},\ldots,0_1,0_0\rangle$, respectively, the composite state at $t=\tau$ is

$$\begin{aligned}|\Psi(\tau)\rangle &= U_{t_{N-1}}\cdots U_{t_0}|\psi_S\rangle \otimes |0_{N-1},\ldots,0_0\rangle \\ &= \sum_{\boldsymbol{m}} V_{m_{N-1}}\cdots V_{m_0}|\psi_S\rangle \otimes |m_{N-1},\ldots,m_0\rangle. \end{aligned} \tag{5}$$

Calculating $\mathrm{Tr}_E[|\Psi(\tau)\rangle\langle\Psi(\tau)|]$ for $\Delta t \to 0$, we recover the original Lindblad equation of Eq. (2). This input-output formalism is referred to as the repeated interaction model in quantum thermodynamics [40–42], which was recently used to derive quantum TURs [43,44]. Importantly, the input-output formalism assumes that the environment is pure so that the time-evolved state in $S+E$ is pure [Eq. (5)], which enables the following calculation. Continuous measurement [45,46] through the environment corresponds to environmental measurement at the final time. When we measure the environment at $t=\tau$ through a set of projectors $\{|\boldsymbol{m}\rangle\langle\boldsymbol{m}|\}_{\boldsymbol{m}}$ with $\boldsymbol{m} \equiv [m_{N-1},\ldots,m_1,m_0]$, we obtain a realization of $\boldsymbol{m}$, and the principal system is projected to $V_{m_{N-1}}\cdots V_{m_0}|\psi_S\rangle$ (note that this is unnormalized). Thus, $\boldsymbol{m}$ comprises a measurement record of continuous measurement. Since the evolution of $V_{m_{N-1}}\cdots V_{m_0}|\psi_S\rangle$ is stochastic depending on the measurement record, it is referred to as a "quantum trajectory," which can be described by the stochastic Schrödinger equation (see Supplemental Material [47]). Figure 2 presents an example of continuous measurement in the input-output formalism for $M=1$ (i.e., a single jump operator) with $N=4$. After the measurement with the set of projectors $\{|\boldsymbol{m}\rangle\langle\boldsymbol{m}|\}_{\boldsymbol{m}}$, suppose we obtain $[1_3, 0_2, 0_1, 1_0]$, where 1's denote the detection of jumps. Then, two jump events occurred in the principal system S in two intervals $[t_0, t_1]$ and $[t_3, t_4]$. Let us define the counting observable $\mathcal{C}$ that counts and weights jump events in a quantum trajectory. We define $\mathcal{C}$ by an Hermitian operator on E, which admits the following eigendecomposition:

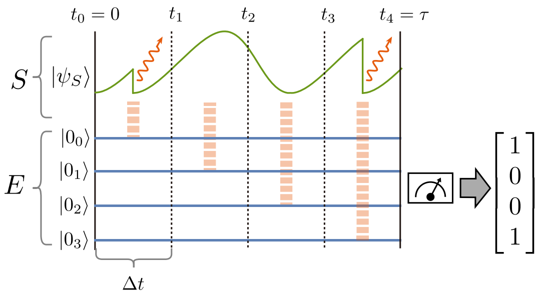

FIG. 2. Illustration of continuous measurement model for $N = 4$. The initial states of S and E are $|\psi_S\rangle$ and $|0_3, 0_2, 0_1, 0_0\rangle$, respectively. The environment subspace $|0_k\rangle$ interacts with S during an interval $[t_k, t_{k+1}]$. Finally, at $t = \tau$, E is measured with a set of projectors $\{|\boldsymbol{m}\rangle\langle\boldsymbol{m}|\}_{\boldsymbol{m}}$. Suppose that the measurement record is $\boldsymbol{m} = [1_3, 0_2, 0_1, 1_0]$. Then, the state of the principal system undergoes two jump events in the intervals $[t_0, t_1]$ and $[t_3, t_4]$.

$$\mathcal{C} = \sum_{\boldsymbol{m}} g(\boldsymbol{m})|\boldsymbol{m}\rangle\langle\boldsymbol{m}| = \sum_c c\Upsilon(c), \tag{6}$$

where $\Upsilon(c) \equiv \sum_{\boldsymbol{m}:g(\boldsymbol{m})=c} |\boldsymbol{m}\rangle\langle\boldsymbol{m}|$ and we assume $g(\boldsymbol{0}) = 0$ with $\boldsymbol{0} \equiv [0_{N-1}, \ldots, 0_1, 0_0]$. A set $\{\Upsilon(c)\}_c$ comprises a projection-valued measure. $g(\boldsymbol{m})$ in Eq. (6) counts and weights jumps in a measurement record $\boldsymbol{m}$. The condition $g(\boldsymbol{0}) = 0$ implies that the counting observable should vanish when there are no jump events, which constitutes a minimum assumption for the counting observable [30]. For instance, $g(\boldsymbol{m})$ is typically expressed as follows:

$$g(\boldsymbol{m}) = \sum_{k=0}^{N-1} C_{m_k}, \tag{7}$$

where $[C_0, C_1, \ldots, C_M]$ with $C_0 = 0$ being a real projection vector specifying the weight of each jump (recall $m_k \in \{0, 1, \ldots, M-1, M\}$). For instance, in Fig. 2 with the weight vector $[C_0, C_1] = [0, 1]$, $g(\boldsymbol{m})$ in Eq. (7) simply counts the number of jumps in $\boldsymbol{m}$ to yield $g(\boldsymbol{m}) = 2$ for $\boldsymbol{m} = [1_3, 0_2, 0_1, 1_0]$. The probability distributions of the counting observable are $\mathbb{P}(c) \equiv \langle\Psi|\mathbb{I}_S \otimes \Upsilon(c)|\Psi\rangle$ and $\mathbb{P}_\star(c) \equiv \langle\Psi_\star|\mathbb{I}_S \otimes \Upsilon(c)|\Psi_\star\rangle$. The mean and standard deviation are $\langle\mathcal{C}\rangle \equiv \langle\Psi(\tau)|\mathbb{I}_S \otimes \mathcal{C}|\Psi(\tau)\rangle = \sum_c c\mathbb{P}(c)$ and $[\![\mathcal{C}]\!] \equiv \sqrt{\langle\mathcal{C}^2\rangle - \langle\mathcal{C}^2\rangle}$, respectively (quantities with a subscript $\star$ should be evaluated for $|\Psi_\star\rangle$ instead of $|\Psi\rangle$).

The Lindblad equation of Eq. (2) covers classical stochastic processes. Consider a classical Markov chain with N_S states. Such classical states can be represented quantum mechanically by an orthonormal basis $\{|b_1\rangle, |b_2\rangle, \ldots, |b_{N_S}\rangle\}$. Classical Markov chains can be emulated by setting $H_S = 0$, $L_{ji} = \sqrt{\gamma_{ji}}|b_j\rangle\langle b_i|$, and $\rho_S(t) = \sum_i p_i(t)|b_i\rangle\langle b_i|$, where γ_{ji} is a transition rate from $|b_i\rangle$ to $|b_j\rangle$, and $p_i(t)$ is the probability of being $|b_i\rangle$ at time t. $\mathcal{C}$ with Eq. (7) is a reminiscent of the counting observable in the classical stochastic thermodynamics, which is defined by $\sum_{j\neq i} \mathsf{C}_{ji}\mathsf{N}_{ji}$ with N_{ji} being the number of transitions from $|b_i\rangle$ to $|b_j\rangle$ in $[0, \tau]$, and $\mathsf{C}_{ji} \in \mathbb{R}$ being its weight. The *current* observable, which is an observable of interest in the conventional TUR [1,2], additionally assumes antisymmetry $\mathsf{C}_{ji} = -\mathsf{C}_{ij}$.

The Loschmidt echo considers the fidelity between the original $|\Psi\rangle$ and perturbed state $|\Psi_\star\rangle$ [Eq. (1)]. Let $H_{\star,S}$ and $L_{\star,m}$ $(1 \le m \le M)$ be the perturbed Hamiltonian and jump operators, respectively, in Eqs. (3) and (4). We define the Kraus operators of the perturbed dynamics $V_{\star,m}$ by Eqs. (3) and (4), where H_S and L_m should be replaced with $H_{\star,S}$ and $L_{\star,m}$, respectively. Similar to Eq. (5), the composite state of the perturbed dynamics at $t = \tau$ is given by

$$|\Psi_\star(\tau)\rangle = \sum_{\boldsymbol{m}} V_{\star,m_{N-1}} \cdots V_{\star,m_0}|\psi_S\rangle \otimes |m_{N-1}, \ldots, m_0\rangle. \tag{8}$$

Calculating the Loschmidt echo $|\langle\Psi_\star|\Psi\rangle|^2$ for Eqs. (5) and (8) is not an easy task since the composite state $[|\Psi(\tau)\rangle$ or $|\Psi_\star(\tau)\rangle]$, comprising the principal system and environment, is generally inaccessible. For continuous measurement, the Loschmidt echo can be explicitly calculated after Refs. [37,49]. Note that $\langle\Psi_\star(t)|\Psi(t)\rangle = \mathrm{Tr}_{SE}[|\Psi(t)\rangle \times \langle\Psi_\star(t)|] = \mathrm{Tr}_S[\phi(t)]$ where $\phi(t) \equiv \mathrm{Tr}_E[|\Psi(t)\rangle\langle\Psi_\star(t)|]$. Thus, using Eqs. (5) and (8), ϕ satisfies a two-sided Lindblad equation [37,49]: $\dot{\phi} = \mathcal{K}\phi \equiv -iH_S\phi + i\phi H_{\star,S} + \sum_m L_m\phi L_{\star,m}^\dagger - \frac{1}{2}\sum_m[L_m^\dagger L_m\phi + \phi L_{\star,m}^\dagger L_{\star,m}]$, where $\mathcal{K}$ is a superoperator. Note that ϕ does not preserve the trace, i.e., $\mathrm{Tr}_S[\phi(t)] \neq 1$ in general. By solving the two-sided Lindblad equation, we obtain $\phi(\tau) = e^{\mathcal{K}\tau}\rho_S(0)$, where $\rho_S(0) = |\psi_S\rangle\langle\psi_S|$ is the initial density operator of the Lindblad dynamics [50]. The Loschmidt echo η is expressed by $\eta = |\mathrm{Tr}_S[e^{\mathcal{K}\tau}\rho_S(0)]|^2$. Importantly, η can be specified by quantities of S alone (H_S, L_m, $H_{\star,S}$, and $L_{\star,m}$). Moreover, the Loschmidt echo $|\langle\Psi_\star|\Psi\rangle|^2$ can be obtained via the consideration of an ancillary qubit [49], which is a natural extension of the approach used to experimentally measure the Loschmidt echo in closed quantum dynamics. The above calculations assumed an initially pure state; however, a generalization to an initially mixed state case is straightforward (see Supplemental Material [47]).

Next, we relate the precision of the counting observable $\mathcal{C}$ with the Loschmidt echo η. Let $\mathcal{F}$ be an arbitrary Hermitian operator on $|\Psi\rangle$ and $|\Psi_\star\rangle$. $\mathcal{F}$ admits the eigendecomposition $\mathcal{F} = \sum_{z\in\mathcal{Z}} z\Lambda(z)$, where $\mathcal{Z}$ and $\Lambda(z)$ represent a set of distinct eigenvalues of $\mathcal{F}$ and a projector corresponding to z, respectively. By using the projector $\Lambda(z)$, the fidelity is bounded from above by

$$|\langle\Psi_\star|\Psi\rangle| \le \sum_{z\in\mathcal{Z}} |\langle\Psi_\star|\Lambda(z)|\Psi\rangle| \le \sum_{z\in\mathcal{Z}} \sqrt{P(z)}\sqrt{P_\star(z)}$$
$$= 1 - \mathcal{H}^2(P, P_\star), \tag{9}$$

where $P(z) \equiv \langle\Psi|\Lambda(z)|\Psi\rangle$, $P_\star(z) \equiv \langle\Psi_\star|\Lambda(z)|\Psi_\star\rangle$, and $\mathcal{H}^2(\bullet,\bullet)$ is the Hellinger distance. The first inequality used the triangle inequality, where the equality holds if and only if the direction of $\langle\Psi_\star|\Lambda(z)|\Psi\rangle$ in the complex plane is the same for all z. The second inequality used the Cauchy-Schwarz inequality, where the equality holds if and only if $\Lambda(z)|\Psi_\star\rangle \propto \Lambda(z)|\Psi\rangle$ for all z. The Hellinger distance is defined as follows: $\mathcal{H}^2(P,P_\star) = \frac{1}{2}\sum_{z\in\mathcal{Z}}(\sqrt{P(z)}-\sqrt{P_\star(z)})^2$, where $0 \le \mathcal{H}^2(P,P_\star) \le 1$. The Hellinger distance has a lower bound, given the mean and variance [51–53]. We use a tighter lower bound recently derived in Refs. [53,54] (see the Supplemental Material [47] for a brief explanation),

$$\mathcal{H}^2(P,P_\star) \ge 1 - \left[\left(\frac{\langle\mathcal{F}\rangle - \langle\mathcal{F}\rangle_\star}{[\![\mathcal{F}]\!] + [\![\mathcal{F}]\!]_\star}\right)^2 + 1\right]^{-\frac{1}{2}}, \quad (10)$$

where $\langle\mathcal{F}\rangle \equiv \langle\Psi|\mathcal{F}|\Psi\rangle = \sum_{z\in\mathcal{Z}} zP(z)$ and $[\![\mathcal{F}]\!] \equiv \sqrt{\langle\mathcal{F}^2\rangle - \langle\mathcal{F}^2\rangle}$ (quantities with a subscript $\star$ should be evaluated for $|\Psi_\star\rangle$ instead of $|\Psi\rangle$). The equality of Eq. (10) holds if and only if $P(z)$ and $P_\star(z)$ are defined on a set consisting of two points. Substituting Eq. (10) into Eq. (9), we obtain

$$\left(\frac{[\![\mathcal{F}]\!] + [\![\mathcal{F}]\!]_\star}{\langle\mathcal{F}\rangle - \langle\mathcal{F}\rangle_\star}\right)^2 \ge \frac{1}{\eta^{-1} - 1}. \quad (11)$$

Note that a similar relation, which is looser than Eq. (11), was derived in Ref. [55]. Because $\mathcal{F}$ is arbitrary, by taking $\mathcal{F} = \mathbb{I}_S \otimes \mathcal{C} = \sum_c c[\mathbb{I}_S \otimes \Upsilon(c)]$ in Eq. (11), where $\mathcal{C}$ is the counting observable defined in Eq. (6), we obtain

$$\left(\frac{[\![\mathcal{C}]\!] + [\![\mathcal{C}]\!]_\star}{\langle\mathcal{C}\rangle - \langle\mathcal{C}\rangle_\star}\right)^2 \ge \frac{1}{|\mathrm{Tr}_S[e^{\mathcal{K}\tau}\rho_S(0)]|^{-2} - 1}, \quad (12)$$

which is the main result of this Letter. The left-hand side of Eq. (12) concerns the counting observable $\mathcal{C}$, whereas the right-hand side can be calculated through H_S, $H_{S,\star}$, L_m, $L_{\star,m}$, and $\rho_S(0)$. The left-hand side of Eq. (12) can be identified as a similarity between two distributions, $\mathbb{P}(c)$ and $\mathbb{P}_\star(c)$, when $(\langle\mathcal{C}\rangle - \langle\mathcal{C}\rangle_\star)^2$ is sufficiently large. Equation (12) shows that the precision of counting observables improves when the extent of irreversibility increases, which qualitatively agrees with the classical TURs [1,2]. Classical TURs have a lower bound based on the entropy production that characterizes the irreversibility of classical Markov processes. Equation (12) is reminiscent of a hysteretic TUR [56], which considers an observable of two processes. Similarly, Eq. (12) includes the mean and variance of two dynamics, the original and perturbed dynamics. The Kraus operators V_m in Eqs. (3) and (4) are not unique; a different Kraus operator corresponds to a different continuous measurement. We can show that Eq. (12) still holds for any continuous measurement (any unraveling) [47]. Let us mention the equality condition of Eq. (12). The equality of Eq. (12) requires the following three conditions: $\langle\Psi_\star|\mathbb{I}_S \otimes \Upsilon(c)|\Psi\rangle$ has the same direction in the complex plane for all c, $[\mathbb{I}_S \otimes \Upsilon(c)]|\Psi_\star\rangle \propto [\mathbb{I}_S \otimes \Upsilon(c)]|\Psi\rangle$ for all c, and $\mathbb{P}(c)$ and $\mathbb{P}_\star(c)$ are defined on a set comprising two points. For instance, an observable that simply counts the number of jumps satisfies the last condition for sufficiently short τ, in which the observable takes either 0 (no jump event) or 1 (one jump event). We perform simulation analysis for Eqs. (12) and numerically verify the bounds (see Supplemental Material [47]). At this point, the condition $g(\mathbf{0}) = 0$ was not used; however, it hereafter plays an important role when considering particular perturbed dynamics.

We consider a specific case of the empty perturbed dynamics in Eq. (12), i.e., $H_{\star,S} = 0$ and $L_{\star,m} = 0$ for all m. Then, the composite state of the perturbed dynamics at $t = \tau$ becomes $|\Psi_\star(\tau)\rangle = |\psi_S\rangle \otimes |0_{N-1},\ldots,0_0\rangle$, which is unchanged from the initial state. In this case, the Loschmidt echo is $\eta = |\langle\Psi(0)|\Psi(\tau)\rangle|^2$. Since $\mathcal{C}$ in Eq. (6) assumes $g(\mathbf{0}) = 0$, $\langle\mathcal{C}\rangle_\star = 0$ and $[\![\mathcal{C}]\!]_\star = 0$ for the empty dynamics. Equation (12) becomes

$$\frac{[\![\mathcal{C}]\!]^2}{\langle\mathcal{C}\rangle^2} \ge \frac{1}{|\mathrm{Tr}_S[e^{-iH_{\mathrm{eff}}\tau}\rho_S(0)]|^{-2} - 1}, \quad (13)$$

where $H_{\mathrm{eff}} \equiv H_S - (i/2)\sum_m L_m^\dagger L_m$ is the effective Hamiltonian (note that H_{eff} is non-Hermitian). Note that Eq. (13) requires continuous measurement that corresponds to Eqs. (3) and (4) [47], whereas Eq. (12) holds for an arbitrary continuous measurement. The bound of Eq. (13) is similar to that obtained in Ref. [30],

$$\frac{[\![\mathcal{C}]\!]^2}{\langle\mathcal{C}\rangle^2} \ge \frac{1}{\mathrm{Tr}_S[e^{-iH_{\mathrm{eff}}^\dagger\tau}\rho_S(0)e^{iH_{\mathrm{eff}}\tau}] - 1}. \quad (14)$$

In the short time limit $\tau \to 0$, Eqs. (13) and (14) reduce to the same bound $[\![\mathcal{C}]\!]^2/\langle\mathcal{C}\rangle^2 \ge 1/\{\mathrm{Tr}_S[\sum_m L_m^\dagger L_m \rho_S(0)]\tau\}$, where the denominator corresponds to the dynamical activity [57] in classical Markov processes. Using the quantum-to-classical mapping explained above, we can obtain a classical limit of Eq. (13) as follows:

$$\frac{[\![\mathcal{C}]\!]^2}{\langle\mathcal{C}\rangle^2} \ge \frac{1}{\left(\sum_i p_i(0)\sqrt{e^{-\tau\sum_{j(\neq i)}\gamma_{ji}}}\right)^{-2} - 1}. \quad (15)$$

Similarly, the classical limit of Eq. (14) is

$$\frac{[\![\mathcal{C}]\!]^2}{\langle\mathcal{C}\rangle^2} \ge \frac{1}{\sum_i e^{\tau\sum_{j(\neq i)}\gamma_{ji}} p_i(0) - 1}, \quad (16)$$

where $e^{-\tau\sum_{j(\neq i)}\gamma_{ji}}$ in Eqs. (15) and (16) corresponds to the probability of no jump within $[0,\tau]$ starting from $|b_i\rangle$, which is an experimentally measurable quantity. By using Jensen's inequality, we can show that Eq. (15) provides a tighter lower bound than Eq. (16). Contrariwise, when the system approaches the closed quantum dynamics, the lower bound of Eq. (14) becomes tighter than that of Eq. (13) (please see Supplemental Material [47] for details).

So far, we have considered the empty perturbed dynamics. We now consider a different perturbed dynamics in Eq. (12), a time-scaled perturbed dynamics. This case is specified by $H_{\star,S} = (1+\varepsilon)H_S$ and $L_{\star,m} = \sqrt{1+\varepsilon}L_m$ for all m, where $\varepsilon \in \mathbb{R}$ is an infinitesimally small parameter. The Lindblad equation of Eq. (2) for the perturbed dynamics becomes $\dot{\rho}_S = (1+\varepsilon)\mathcal{L}\rho_S$, which is identical to the original dynamics, except for its timescale. Assume that this Lindblad equation converges to a single steady-state density operator. Moreover, we perform a continuous measurement corresponding to Eqs. (3) and (4) assuming the condition of Eq. (7) for the counting observable. Then, for $\tau \to \infty$, according to Ref. [58], the mean and variance of the perturbed dynamics satisfy $\langle \mathcal{C} \rangle_\star = (1+\varepsilon)\langle \mathcal{C} \rangle$ and $[\![\mathcal{C}]\!]_\star^2 = (1+\varepsilon)[\![\mathcal{C}]\!]^2$ [47]. This scaling relation is intuitive; since the timescale of the perturbed dynamics is $1+\varepsilon$ times faster (when $\varepsilon > 0$), jump events occur $1+\varepsilon$ times more frequently within the fixed time interval $[0, \tau]$ for $\tau \to \infty$. However, this scaling relation does not necessarily hold with a different continuous measurement. The left-hand side of Eq. (12) becomes $(1+\sqrt{1+\varepsilon})^2 [\![\mathcal{C}]\!]^2 / (\varepsilon^2 \langle \mathcal{C} \rangle^2)$. Since $|\Psi_\star(\tau)\rangle$ depends on ε, we may write $|\Psi_\star(\tau)\rangle = |\Psi(\tau;\varepsilon)\rangle$, where $|\Psi(\tau)\rangle = |\Psi(\tau;\varepsilon=0)\rangle$ because $\varepsilon = 0$ case reduces to the original dynamics. Next, we evaluate the right-hand side of Eq. (12). The fidelity and quantum Fisher information are related via [59]

$$\mathcal{J}(\tau) = \frac{8}{\varepsilon^2}[1 - |\langle \Psi(\tau;\varepsilon)|\Psi(\tau;0)\rangle|] \quad (\varepsilon \to 0), \qquad (17)$$

where $\mathcal{J}(\tau)$ denotes the quantum Fisher information [60–63]. Substituting the scaling relation of the left-hand side and Eq. (17) into Eq. (12), for $\varepsilon \to 0$, we obtain

$$\frac{[\![\mathcal{C}]\!]^2}{\langle \mathcal{C} \rangle^2} \geq \frac{1}{\mathcal{J}(\tau)} \quad (\tau \to \infty). \qquad (18)$$

Equation (18) rederives a quantum TUR obtained in Ref. [28] through the quantum Cramér-Rao inequality [60–63]. In Ref. [28], $\mathcal{J}(\tau)$ was explicitly evaluated and shown to reduce to dynamical activity in the classical limit. $\mathcal{J}(\tau)$ linearly depends on τ, which contrasts with Eq. (13). Therefore, a classical TUR comprising dynamical activity [6] can be derived as a particular case of Eq. (12). Since Eqs. (18) and (13) depend on τ linearly and exponentially, respectively, Eq. (18) is tighter than Eq. (13). However, Eq. (13) requires fewer assumptions on the dynamics and observable; Eq. (13) holds for arbitrary dynamics and for counting observables satisfying $g(\mathbf{0}) = 0$, whereas Eq. (18) is valid only for steady-state dynamics ($\tau \to \infty$) and for the counting observable, which satisfies the additional assumption given in Eq. (7). The relative entropy between two nearby probability distributions yields the Fisher information, which plays a fundamental role in classical stochastic thermodynamics [10,64–66]. Contrariwise, the quantum relative entropy between two nearby density operators does *not* yield the quantum Fisher information [67], but the fidelity does [Eq. (17)], which indicates that not the quantum relative entropy, but the Loschmidt echo, provides a unified perspective on classical and quantum TURs.

Conclusion.—In this Letter, we obtained a relation between the Loschmidt echo and the precision of continuous measurement in quantum Markov processes, which can be viewed as a quantum generalization of classical TURs. Since the relations derived in this Letter exploited the advantage of general quantum bounds, which holds for general Hermitian operators, we can obtain other thermodynamic relations for the continuous measurement through our approach. Indeed, in our followup paper [68], we obtain a TUR for quantum first passage processes using the same technique. Moreover, because Eq. (12) shows that the upper bound of the Loschmidt echo $|\langle \Psi_\star | \Psi \rangle|^2$ can be obtained from the continuous measurement, a possible application of Eq. (12) is related to thermodynamic inference, which is actively studied in classical TURs [69–72].

This work was supported by the Ministry of Education, Culture, Sports, Science and Technology (MEXT) KAKENHI Grant No. JP19K12153.

*hasegawa@biom.t.u-tokyo.ac.jp

[1] A. C. Barato and U. Seifert, Thermodynamic Uncertainty Relation for Biomolecular Processes, Phys. Rev. Lett. **114**, 158101 (2015).
[2] T. R. Gingrich, J. M. Horowitz, N. Perunov, and J. L. England, Dissipation Bounds All Steady-State Current Fluctuations, Phys. Rev. Lett. **116**, 120601 (2016).
[3] P. Pietzonka, A. C. Barato, and U. Seifert, Universal bounds on current fluctuations, Phys. Rev. E **93**, 052145 (2016).
[4] J. M. Horowitz and T. R. Gingrich, Proof of the finite-time thermodynamic uncertainty relation for steady-state currents, Phys. Rev. E **96**, 020103(R) (2017).
[5] S. Pigolotti, I. Neri, E. Roldán, and F. Jülicher, Generic Properties of Stochastic Entropy Production, Phys. Rev. Lett. **119**, 140604 (2017).
[6] J. P. Garrahan, Simple bounds on fluctuations and uncertainty relations for first-passage times of counting observables, Phys. Rev. E **95**, 032134 (2017).
[7] A. Dechant and S.-i. Sasa, Current fluctuations and transport efficiency for general Langevin systems, J. Stat. Mech. (2018) 063209.
[8] A. C. Barato, R. Chetrite, A. Faggionato, and D. Gabrielli, Bounds on current fluctuations in periodically driven systems, New J. Phys. **20**, 103023 (2018).

[9] I. D. Terlizzi and M. Baiesi, Kinetic uncertainty relation, J. Phys. A **52**, 02LT03 (2019).

[10] Y. Hasegawa and T. Van Vu, Uncertainty relations in stochastic processes: An information inequality approach, Phys. Rev. E **99**, 062126 (2019).

[11] Y. Hasegawa and T. Van Vu, Fluctuation Theorem Uncertainty Relation, Phys. Rev. Lett. **123**, 110602 (2019).

[12] T. Van Vu and Y. Hasegawa, Uncertainty relations for underdamped Langevin dynamics, Phys. Rev. E **100**, 032130 (2019).

[13] T. Van Vu and Y. Hasegawa, Thermodynamic uncertainty relations under arbitrary control protocols, Phys. Rev. Research **2**, 013060 (2020).

[14] A. Dechant and S.-i. Sasa, Fluctuation-response inequality out of equilibrium, Proc. Natl. Acad. Sci. U.S.A. **117**, 6430 (2020).

[15] V. T. Vo, T. Van Vu, and Y. Hasegawa, Unified approach to classical speed limit and thermodynamic uncertainty relation, Phys. Rev. E **102**, 062132 (2020).

[16] T. Koyuk and U. Seifert, Thermodynamic Uncertainty Relation for Time-Dependent Driving, Phys. Rev. Lett. **125**, 260604 (2020).

[17] A. Dechant and S. ichi Sasa, Continuous time-reversal and equality in the thermodynamic uncertainty relation, Phys. Rev. Research **3**, L042012 (2021).

[18] J. M. Horowitz and T. R. Gingrich, Thermodynamic uncertainty relations constrain non-equilibrium fluctuations, Nat. Phys. **16**, 15 (2019).

[19] A. Peres, Stability of quantum motion in chaotic and regular systems, Phys. Rev. A **30**, 1610 (1984).

[20] T. Gorin, T. Prosen, T. H. Seligman, and M. Žnidarič, Dynamics of Loschmidt echoes and fidelity decay, Phys. Rep. **435**, 33 (2006).

[21] A. Goussev, R. A. Jalabert, H. M. Pastawski, and D. Wisniacki, Loschmidt echo, Scholarpedia **7**, 11687 (2012).

[22] P. Erker, M. T. Mitchison, R. Silva, M. P. Woods, N. Brunner, and M. Huber, Autonomous Quantum Clocks: Does Thermodynamics Limit Our Ability to Measure Time?, Phys. Rev. X **7**, 031022 (2017).

[23] K. Brandner, T. Hanazato, and K. Saito, Thermodynamic Bounds on Precision in Ballistic Multiterminal Transport, Phys. Rev. Lett. **120**, 090601 (2018).

[24] F. Carollo, R. L. Jack, and J. P. Garrahan, Unraveling the Large Deviation Statistics of Markovian Open Quantum Systems, Phys. Rev. Lett. **122**, 130605 (2019).

[25] J. Liu and D. Segal, Thermodynamic uncertainty relation in quantum thermoelectric junctions, Phys. Rev. E **99**, 062141 (2019).

[26] G. Guarnieri, G. T. Landi, S. R. Clark, and J. Goold, Thermodynamics of precision in quantum nonequilibrium steady states, Phys. Rev. Research **1**, 033021 (2019).

[27] S. Saryal, H. M. Friedman, D. Segal, and B. K. Agarwalla, Thermodynamic uncertainty relation in thermal transport, Phys. Rev. E **100**, 042101 (2019).

[28] Y. Hasegawa, Quantum Thermodynamic Uncertainty Relation for Continuous Measurement, Phys. Rev. Lett. **125**, 050601 (2020).

[29] H. M. Friedman, B. K. Agarwalla, O. Shein-Lumbroso, O. Tal, and D. Segal, Thermodynamic uncertainty relation in atomic-scale quantum conductors, Phys. Rev. B **101**, 195423 (2020).

[30] Y. Hasegawa, Thermodynamic Uncertainty Relation for General Open Quantum Systems, Phys. Rev. Lett. **126**, 010602 (2021).

[31] M. F. Sacchi, Thermodynamic uncertainty relations for bosonic Otto engines, Phys. Rev. E **103**, 012111 (2021).

[32] Alex Arash Sand Kalaee, A. Wacker, and P. P. Potts, Violating the thermodynamic uncertainty relation in the three-level maser, Phys. Rev. E **104**, L012103 (2021).

[33] A. M. Timpanaro, G. Guarnieri, and G. T. Landi, The most precise quantum thermoelectric, arXiv:2106.10205.

[34] G. Lindblad, On the generators of quantum dynamical semigroups, Commun. Math. Phys. **48**, 119 (1976).

[35] H.-P. Breuer and F. Petruccione, *The Theory of Open Quantum Systems* (Oxford University Press, New York, 2002).

[36] M. Guţă, Fisher information and asymptotic normality in system identification for quantum Markov chains, Phys. Rev. A **83**, 062324 (2011).

[37] S. Gammelmark and K. Mølmer, Fisher Information and the Quantum Cramér-Rao Sensitivity Limit of Continuous Measurements, Phys. Rev. Lett. **112**, 170401 (2014).

[38] K. Macieszczak, M. Guţă, I. Lesanovsky, and J. P. Garrahan, Dynamical phase transitions as a resource for quantum enhanced metrology, Phys. Rev. A **93**, 022103 (2016).

[39] J. A. Gross, C. M. Caves, G. J. Milburn, and J. Combes, Qubit models of weak continuous measurements: Markovian conditional and open-system dynamics, Quantum Sci. Technol. **3**, 024005 (2018).

[40] J. M. Horowitz and J. M. R. Parrondo, Entropy production along nonequilibrium quantum jump trajectories, New J. Phys. **15**, 085028 (2013).

[41] G. Manzano, J. M. Horowitz, and J. M. R. Parrondo, Quantum Fluctuation Theorems for Arbitrary Environments: Adiabatic and Nonadiabatic Entropy Production, Phys. Rev. X **8**, 031037 (2018).

[42] J. Santos, A. Timpanaro, and G. Landi, Joint fluctuation theorems for sequential heat exchange, Entropy **22**, 763 (2020).

[43] H. J. D. Miller, M. H. Mohammady, M. Perarnau-Llobet, and G. Guarnieri, Thermodynamic Uncertainty Relation in Slowly Driven Quantum Heat Engines, Phys. Rev. Lett. **126**, 210603 (2021).

[44] H. J. D. Miller, M. H. Mohammady, M. Perarnau-Llobet, and G. Guarnieri, Joint statistics of work and entropy production along quantum trajectories, Phys. Rev. E **103**, 052138 (2021).

[45] H. M. Wiseman, Quantum trajectories and quantum measurement theory, J. Eur. Opt. Soc. Part B **8**, 205 (1996).

[46] C. Elouard and M. H. Mohammady, Work, heat and entropy production along quantum trajectories, in *Thermodynamics in the Quantum Regime: Fundamental Aspects and New Directions*, edited by F. Binder, L. A. Correa, C. Gogolin, J. Anders, and G. Adesso (Springer International Publishing, Cham, 2018), pp. 363–393.

[47] See Supplemental Material at http://link.aps.org/supplemental/10.1103/PhysRevLett.127.240602 for details of calculations, which includes Ref. [48].

[48] G. T. Landi, Quantum information and quantum noise, University of São Paulo Technical Report, 2018, http://www.fmt.if.usp.br/~gtlandi/quantum-information-and.html.

[49] K. Mølmer, Hypothesis Testing with Open Quantum Systems, Phys. Rev. Lett. **114**, 040401 (2015).

[50] Since $\mathcal{K}$ is a superoperator, evaluating $e^{\mathcal{K}\tau}$ requires the calculation in the Liouville space [47].

[51] M. Dashti and A. M. Stuart, The Bayesian approach to inverse problems, in Handbook of Uncertainty Quantification, edited by R. Ghanem, D. Higdon, and H. Owhadi (Springer, Cham, 2017), pp. 311–428.

[52] M. A. Katsoulakis, L. Rey-Bellet, and J. Wang, Scalable information inequalities for uncertainty quantification, J. Comput. Phys. **336**, 513 (2017).

[53] T. Nishiyama, A tight lower bound for the Hellinger distance with given means and variances, arXiv:2010.13548.

[54] T. Nishiyama and I. Sason, On relations between the relative entropy and χ^2-divergence, generalizations and applications, Entropy **22**, 563 (2020).

[55] A. S. Holevo, A generalization of the Rao-Cramér inequality, Teor. Veroyatn. Ee Primen. **18**, 359 (1973).

[56] K. Proesmans and J. M. Horowitz, Hysteretic thermodynamic uncertainty relation for systems with broken time-reversal symmetry, J. Stat. Mech. (2019) 054005.

[57] C. Maes, Frenesy: Time-symmetric dynamical activity in nonequilibria, Phys. Rep. **850**, 1 (2020).

[58] D. Burgarth, V. Giovannetti, A. N. Kato, and K. Yuasa, Quantum estimation via sequential measurements, New J. Phys. **17**, 113055 (2015).

[59] S. L. Braunstein and C. M. Caves, Statistical Distance and the Geometry of Quantum States, Phys. Rev. Lett. **72**, 3439 (1994).

[60] C. W. Helstrom, *Quantum Detection and Estimation Theory* (Academic Press, New York, 1976).

[61] M. Hotta and M. Ozawa, Quantum estimation by local observables, Phys. Rev. A **70**, 022327 (2004).

[62] M. G. A. Paris, Quantum estimation for quantum technology, Int. J. Quantum. Inform. **07**, 125 (2009).

[63] J. Liu, H. Yuan, X.-M. Lu, and X. Wang, Quantum Fisher information matrix and multiparameter estimation, J. Phys. A **53**, 023001 (2020).

[64] A. Dechant, Multidimensional thermodynamic uncertainty relations, J. Phys. A **52**, 035001 (2019).

[65] S. Ito and A. Dechant, Stochastic Time Evolution, Information Geometry, and the Cramér-Rao Bound, Phys. Rev. X **10**, 021056 (2020).

[66] S. B. Nicholson, L. P. Garcia-Pintos, A. del Campo, and J. R. Green, Time-information uncertainty relations in thermodynamics, Nat. Phys. **16**, 1211 (2020).

[67] H. Nagaoka, On the relation between Kullback divergence and Fisher information: From classical systems to quantum systems, in Asymptotic Theory of Quantum Statistical Inference (World Scientific, Singapore, 2005), pp. 399–419.

[68] Y. Hasegawa, Thermodynamic uncertainty relation for quantum first passage process via Loschmidt echo, arXiv:2106.09870.

[69] J. Li, J. M. Horowitz, T. R. Gingrich, and N. Fakhri, Quantifying dissipation using fluctuating currents, Nat. Commun. **10**, 1666 (2019).

[70] S. K. Manikandan, D. Gupta, and S. Krishnamurthy, Inferring Entropy Production from Short Experiments, Phys. Rev. Lett. **124**, 120603 (2020).

[71] T. Van Vu, V. T. Vo, and Y. Hasegawa, Entropy production estimation with optimal current, Phys. Rev. E **101**, 042138 (2020).

[72] S. Otsubo, S. Ito, A. Dechant, and T. Sagawa, Estimating entropy production by machine learning of short-time fluctuating currents, Phys. Rev. E **101**, 062106 (2020).